Astron. Astrophys. 282, 955–979 (1994)

ASTRONOMY
AND
ASTROPHYSICS

Delivery of meteorites through the ν_6 secular resonance

A. Morbidelli[1], R. Gonczi[1], Ch. Froeschlé[2], and P. Farinella[2,3]

[1] Observatoire de la Côte d'Azur, Dept. CERGA, B.P. 229, F-06304 Nice Cedex 4, France
[2] Observatoire de la Côte d'Azur, Dept. Cassini, B.P. 229, F-06304 Nice Cedex 4, France
[3] Gruppo di Meccanica Spaziale, Dipartimento di Matematica, Università di Pisa, Via Buonarroti 2, I-56127 Pisa, Italy

Received 29 July 1993 / Accepted 2 September 1993

Abstract. The ν_6 secular resonance provides an effective inner and high–inclination boundary to the main asteroid belt in the proper element space, as objects inserted into it can undergo drastic secular changes of eccentricity and become Mars– and Earth–crossers. We have used Morbidelli's (1993) theory for the secular evolution of the orbits lying inside the resonance and Farinella's et al. (1993a) model for the isotropic ejection of fragments following collisions against existing main–belt asteroids, to study the efficiency of 20 asteroids close to the ν_6 resonance as potential deliverers of planet–crossing fragments. We have found that several of these asteroids do inject into the resonance a significant fraction of their fragments, which then have their orbital eccentricities increased up to Mars– and even Earth–crossing values. Therefore some of these bodies — in particular the largest ones, like 6 Hebe, 304 Olga, 739 Mandeville and 759 Vinifera — are probably efficient deliverers of meteorites. The time required for these fragments to be transported into Earth–crossing orbits is typically of the order of 10^6 yr when the eccentricity is directly pumped up by the resonance to ≈ 0.6, longer when Mars encounters are needed as an intermediate process. Other asteroids inject a substantial fraction of their fragments into the 3/1 (623 Chimaera, 1892 Lucienne) and 5/2 (631 Philippina, 907 Rhoda, 1222 Tina) Kirkwood gaps. All these asteroids should become the targets of detailed spectrophotometric investigations, to assess their similarity to some of the known meteorite types.

Key words: celestial mechanics – minor planets – meteoroids

1. Introduction

During the recent history of the Earth, some 10^8 kg/yr of meteoritic material has been falling onto it, ranging in size from microscopic dust to 10–km diameter asteroids (Ceplecha 1992). Where does this material come from? Until two centuries ago, the fall of stones from the sky was believed by scientists to be an absurd and impossible occurrence; later on, on the other hand, meteorites were long believed to be interstellar objects travelling on hyperbolic heliocentric orbits. Today, the birthplace of meteorites has been recognized to lie in the main asteroid belt, where the growth of a full–sized planet was aborted during the early evolution of the solar system. However, until recently serious problems remained in understanding the asteroid–meteorite connection. As a consequence of interasteroidal impact events, fragments are usually ejected from their parent bodies at velocities of the order of 100 – 200 m/s (Zappalà et al. 1984, 1990; Bendjoya et al. 1991), too small for directly causing the drastic orbital changes needed to achieve planet–crossing orbits. On the other hand, impulsive velocity increments of several km/s would normally induce in the meteoritic material strong shock and thermal modifications, which are seldom observed. Thus the interplay between collisions and subtle resonant effects is required to transport material from the asteroid belt to the Earth.

A long–standing issue in planetary science is related to the efficiency of these dynamical routes leading meteorites and Near-Earth Asteroids (NEAs) from the main asteroid belt — where they originated as fragments of larger objects — to orbits allowing close Earth encounters (and collisions). In the last decade many studies have focused on these delivery mechanisms. Wisdom (1983, 1985) showed that the semimajor axis interval between 2.48 and 2.52 AU, where the Kirkwood gap corresponding to the 3/1 mean motion commensurability with Jupiter is located, includes a large chaotic region, possibly causing strong eccentricity increases on time scales $\leq 10^6$ yr. This result was used by Wetherill (1985, 1987) to argue that the 3/1 mean motion resonance provides the most important source of ordinary chondrites. On the basis of his Monte Carlo model of orbital evolution , Wetherill showed that asteroid collisional debris produced at the borders of the 3/1 gap with ejection velocities between 50 and 200 m/s has a high probability to be placed into the chaotic region; there the resonance pumps up the orbital eccentricity to ≈ 0.6, corresponding to a perihelion distance of about 1 AU, and later on close encounters with the Earth, removing the semimajor axis from the resonant range, give raise to a typical Earth–crossing orbit. Besides the 3/1 Kikwood gap, Wetherill also suggested that another possible source

Send offprint requests to: Ch. Froeschlé of meteorites lies in the innermost asteroid belt, at semimajor axes between 2.0 and 2.25 AU, thanks to the presence of the secular resonance ν_6 (or $g = g_6$) which provides the inner and high–inclination boundary to the observed asteroid distribution (Williams 1969; Williams & Faulkner 1981). Numerical computations by Scholl & Froeschlé (1991) showed that indeed in this zone the ν_6 secular resonance, often acting in a synergistic way with the 4/1 mean motion resonance with Jupiter, gives raise to a fairly broad region where Earth–crossing chaotic orbits are generated. Moreover, Yoshikawa (1987), Scholl et al. (1989), Kneževič et al. (1991) and Froeschlé & Scholl (1992) showed that the ν_6 resonance is probably an efficient fragment collector not only near the inner edge of the belt, but also in the moderate–inclination (15° to 20°) regions at semimajor axes of about 2.4 and 2.7 AU.

Subsequent work by our group (Farinella et al. 1993a,b) has shown that plausible collisional physics and dynamical mechanisms can easily generate significant numbers of Earth–crossing asteroid fragments. The ejection of fragments from cratering or break–up events involving thousands of numbered main–belt asteroids having semimajor axes inside 2.8 AU has been simulated through a numerical model, consistent with the experimental results on the outcomes of high–velocity ($\approx$ 5 km/s) impacts (Davis et al. 1989; Petit & Farinella 1993). For every asteroid, the flux of fragments dropped into the chaotic regions of the phase space associated with the 3/1 and ν_6 resonances has been estimated, providing indications about the most effective potential meteorite–delivering asteroids (Farinella et al. 1993a). Several fictitious fragments whose orbits have been integrated for a few millions years have displayed orbital evolution patterns closely resembling those of real NEAs and of the largest observed fireballs, such as that associated with the Příbram meteorite fall (Farinella et al. 1993b). Also, we have estimated the NEA/meteorite production potential of the massive fragment ejection events which generated some populous asteroid families — in particular, very interesting results have been obtained for the case of Vesta, in which recent spectrophotometrie observations by Binzel & Xu (1993) have indicated a clear genetic relationship between a large main–belt asteroid, a number of minor family members lying close to it in the proper element space, a few km–sized NEAs and a specific meteorite type (the basaltic achondrites).

However, our results also showed that as far as the ν_6 resonance is concerned, the criterion used by Farinella et al. (1993a) to assess which ones among the fictitious fragments were injected *inside* the resonance and then were subjected to strong eccentricity increases, was very rough. There are several reasons for that: (i) the resonance position may not have been estimated accurately enough, especially near the mean motion resonances; (ii) the width of the phase space strip where the eccentricity is pumped up by the resonance was just guessed at (actually, it was an input parameter of the model); (iii) the positions in the proper element space of both the target asteroids and the fictitious fragments were subject to some uncertainty, as the proximity to a strong secular resonance can degrade the accuracy of the algorithm computing the proper elements; and (iv) even asteroids placed in the resonance may just undergo small–amplitude librations and avoid large eccentricity changes (a few cases of this type have been discussed by Froeschlé & Scholl 1987; Morbidelli & Henrard 1991). Actually, the numerical integrations by Farinella et al. (1993b) of fictitious fragments from the large asteroid 6 Hebe, located close to the ν_6 resonance at a semimajor axis of 2.42 AU, showed that only 4 over 16 bodies predicted to lie in the resonant strip became Earth–crossers in a time span of the order of 1 Myr. Thus, the real efficiency of the ν_6 route from the asteroid belt to the Earth should be tested by a method suited to explore systematically the relevant part of the phase space — namely, by a semianalytical theory, much faster than N–body numerical experiments in assessing the long–term ($\approx$ 1 Myr) behavior of a large number (tens of thousands) of test bodies.

Such a theory, capable of predicting in a quantitative way the dynamical evolution of any small body located inside or close to a secular resonance, has been recently developed and tested against numerical integrations by one of us (Morbidelli 1993). It looks particularly suitable for the present study, since it takes less than 1 minute of CPU time on a HP720 computer to obtain a prediction for the long–term behavior of a resonant or near–resonant object, while a numerical integration over 1 Myr takes approximatively 10 hours of CPU time on the same computer. Therefore, we are now going to apply this technique to study in a statistical fashion the dynamical behavior of fragments ejected from cratering or break–up events undergone by a number of real asteroids, located near the ν_6 secular resonance. This will hopefully refine our insight into the way asteroid fragments can be injected into Earth–crossing orbits, and will help identifying the most promising candidate meteorite parent bodies.

The remainder of this paper is organized as follows. In Sect. 2 we recall briefly the fragment production and resonance injection model, which has been partially modified with respect to that used by Farinella (1993a,b). Section 3 summarizes Morbidelli's (1993) algorithm to derive resonant proper elements and to assess the long–term behavior of resonant or near–resonant test bodies. In Sect. 4 we describe the results obtained when this technique is applied to fictitious fragments ejected from a number of real asteroids, lying close to the resonance strip. Some conclusions and possible developments of this work are discussed in Sect. 5.

2. The fragmentation/injection model

Since we were interested in the efficiency of fragment delivery through the ν_6 secular resonance, we selected 20 real asteroids that are located near the resonance according to the results of Farinella et al. (1993a) and Morbidelli (1993). Their osculating elements have been taken from the Leningrad Ephemerides for 1993, and refer to JD 244900. These bodies are listed in Table 1, together with their mean elements (Milani & Kneževič 1990, 1992). Since we wanted to simulate the collisional ejection of fragments occurring at random times during a total interval exceeding 10^6 yr, we first integrated numerically the orbit of each asteroid over one half of the circulation period of the secular argument which characterizes the ν_6 resonance, $\varpi - \varpi_S$ (lon-

Table 1. Mean elements for the 20 asteroids close to the ν_6 resonance whose fragments have been studied in this paper. The columns give number, argument of perihelion, nodal longitude, inclination, eccentricity and semimajor axis of each asteroid, and also the initial and final time (starting from the present epoch) of the interval over which their orbits have been numerically integrated

No.	$\omega°$	$\Omega°$	$i°$	e	$a(AU)$	$t_{\min}(10^3$y)	$t_{\max}(10^3$y)
6	235.3	138.9	13.438	0.202	2.4253	100	280
304	166.9	160.4	14.891	0.221	2.4036	250	550
623	126.9	303.0	15.654	0.113	2.4603	0	150
631	273.6	225.5	19.678	0.083	2.7927	0	180
739	41.6	135.6	19.330	0.142	2.7376	0	200
759	2.8	313.0	21.304	0.206	2.6176	0	300
907	91.2	35.9	18.917	0.162	2.8008	0	100
930	333.8	333.3	16.304	0.144	2.4310	0	1000
963	14.2	50.0	6.960	0.138	2.2477	30	170
1222	55.6	245.7	20.884	0.250	2.7913	0	600
1468	25.5	302.7	11.433	0.270	2.1957	0	1000
1892	95.6	309.7	15.394	0.089	2.4617	50	210
1916	340.6	332.2	13.848	0.449	2.2727	0	250
2033	139.4	313.2	9.809	0.111	2.2253	0	200
2368	42.2	284.2	6.826	0.412	2.1053	0	1000
2548	291.7	295.4	19.698	0.101	2.6331	0	600
2604	132.4	121.5	13.320	0.232	2.3879	300	510
3402	318.6	339.2	5.578	0.279	2.1318	0	400
3833	166.5	173.8	11.355	0.388	2.1957	0	500
4095	77.1	264.7	3.947	0.118	2.1201	0	550

gitude of perihelion of the asteroid minus that of Saturn). This corresponds to a time span of the order of a few times 10^5 yr; for the objects which were found librating *inside* the resonance or whose orbital evolution was strongly chaotic, we anyway took an integration time span of similar length — see Table 1, where for each object we have listed the initial and final integration times (starting from the present epoch). Then we chose at random 100 epochs within the integration time spans, corresponding to different osculating elements of the asteroid, and in each case we simulated the isotropic ejection (and escape) of 10 fragments following an impact, according to the model summarized below. Thus we analyzed the dynamical behavior of 10^3 fictitious fragments for each one of the 20 considered asteroids.

Our fragment ejection model is basically the same used in Farinella et al. (1993a,b). The ejection from the parent asteroid was assumed to be isotropic, namely the direction of the fragment ejection velocity vector was taken at random; while this is of course not the case for any single collisional event, it is a reasonable assumption when one averages over a large number of independent events. The magnitude of the ejection velocity V_{ej} was assumed to follow a truncated power–law distribution with a lower cutoff (this is a reasonable approximation of the distributions found in laboratory experiments on hypervelocity impacts), so that the number of fragments ejected having speeds in the interval $(V_{ej}, V_{ej} + dV_{ej})$ is

$$dN(V_{ej}) = C\, V_{ej}^{-\alpha}\, dV_{ej}\ , \qquad (1)$$

for $V_{ej} > V_{min}$, while $dN(V_{ej}) = 0$ for $V_{ej} < V_{min}$ (implying that V_{min} is the lower–cutoff velocity). C is a normalization constant. For the exponent α we adopted the value 3.25, which is roughly consistent with experimental results for both cratering and break–up events (note that the total kinetic energy of the fragments is finite only provided $\alpha > 3$). Provided $\alpha > 2$, the mean value of the distribution is $\frac{(\alpha-1)}{(\alpha-2)} V_{min}$ (= $1.8\, V_{min}$ for $\alpha = 3.25$). In our "nominal" case we took V_{min} = 100 m/s, but in the case of 6 Hebe we tested also the value 200 m/s. These values match the range inferred for asteroid families from

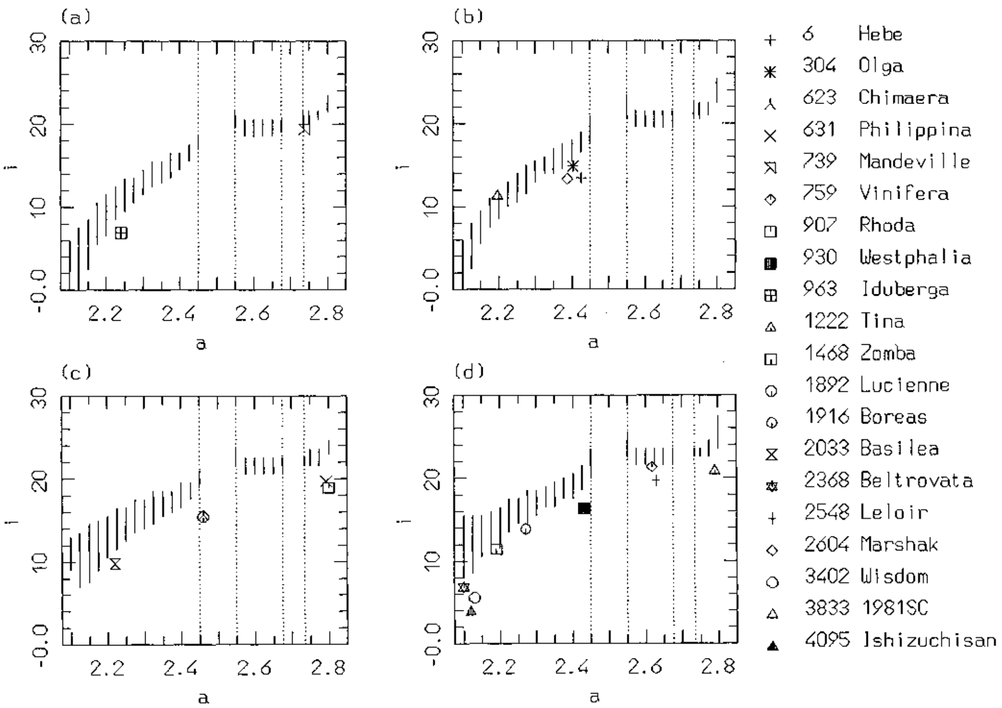

Fig. 1. a–d. The positions of the 20 asteroids analyzed in this paper in the mean inclination i (degrees) vs. mean semimajor axis a (AU) plane. The dashed strips appearing in the four diagrams correspond to initial conditions leading to a maximum eccentricity > 0.4. These strips have been derived by using a grid with steps 1° in i and 0.025 AU in a, for a mean eccentricity $e = 0.15$ and mean values of the argument of perihelion ω and nodal longitude Ω equal to $\omega = 0°, \Omega = 124°.19$ **a**; $\omega = 180°, \Omega = 124°.19$ **b**; $\omega = 180°, \Omega = 304°.19$ **c**; $\omega = 0°, \Omega = 304°.19$ **d**. These values correspond to the critical argument of the ν_6 resonance $\sigma = 0°$ **a**, 180° **b**, 0° **c** and 180° **d**. Two gaps surround the 3/1 and 8/3 mean motion resonances, in the vicinity of which the theory does not work. The asteroids have been plotted in the diagram corresponding to the choice of ω and Ω closest to their actual values.

the escape velocity of their largest members and the observed dispersion of proper elements (Zappalà et al. 1984, 1990).

For every asteroid, from the diameter D we then computed the escape velocity $V_{esc} = (60\,\mathrm{m/s})(D/100\,\mathrm{km})$, corresponding to a density of about 2.5 g/cm^3. Each fragment was tested to check whether $V_{ej} > V_{esc}$, and if so was assumed to escape "to infinity" with a final velocity $V = (V_{ej}^2 - V_{esc}^2)^{1/2}$. It is easy to show that the distribution of the relative velocity "at infinity" V is given by:

$$dN(V) = CV(V^2 + V_{esc}^2)^{-(\alpha+1)/2}\, dV\ , \qquad (2)$$

for $V_{min} < V_{esc}$; otherwise, the distribution is given by Eq.(2) only for $V > (V_{min}^2 - V_{esc}^2)^{1/2}$, while $dN = 0$ for lower velocities. The peak of (2) occurs at $V = V_{esc}/\sqrt{\alpha}$, namely at a relative velocity smaller than, but comparable to the target's escape velocity; however, this is true only provided $V_{min} < V_{esc}$.

3. Short description of the resonant proper element algorithm

This section is devoted to a brief explanation of the algorithm for the computation of the secular resonant dynamics (e.g. resonant proper elements). This algorithm has been illustrated in detail in Morbidelli (1993), where many comparisons with numerical integrations are also provided; moreover in the same paper an analysis is reported on the dynamical behavior of most of the parent asteroids considered here.

The model for the computation of the secular resonant evolution of asteroid orbits takes into account the perturbation effects of Jupiter and Saturn. The Hamiltonian of the problem is averaged with respect to the mean longitudes of the asteroid and the planets, provided they are not in a mean motion resonant configuration. The averaging operation introduces, following the Lie algorithm, terms of higher order in the perturbing masses of the planets; only the quadratic term in the mass of Jupiter is taken into account. The averaged Hamiltonian is computed without any expansion in power series of the eccentricity and the inclination of the asteroid, in order to have an accurate model also for large values of these variables. The Hamiltonian and its derivatives are stocked once for ever in a three dimensional grid in the $a - e - i$ space (see Lemaître & Morbidelli 1993). By spline interpolation one then computes the Hamiltonian at any desired point of the phase space.

The averaged Hamiltonian is expanded in power series of the eccentricity and inclination of the planets, which are small and therefore assumed as perturbation parameters. Then, only the linear terms in (e', i') (the $'$ symbol referring to the planets) are retained, consistently with the perturbation approach adopted, which is a first order one. With these settings, the secular Hamiltonian K is split into $K_0 + K_1$, where K_0 is the averaged perturbation caused by the planets, assumed to be on coplanar circular orbits, and K_1 is the linear part in (e', i').

It is easy to prove (Kozai 1962) that K_0 is a two–degrees of freedom integrable Hamiltonian, although its dynamics is not trivial. In particular, at a critical inclination ($\approx$ 35 degrees in the asteroid belt) the argument of perihelion can librate, while, at lower inclination, the argument of perihelion always circulates. On the other hand, K_1 is time dependent, since it depends on the

Table 2. For each asteroid, the Table gives the diameter, the taxonomic type and the percentages of fragments injected into the 3/1 and 5/2 mean motion resonances and achieving Mars– or Earth–crossing orbits due to ν_6 resonant perturbations. Fragments from asteroid 6 Hebe were generated twice, with V_{min} = 100 m/s (6a) and 200 m/s (6b)

No.	D (km)	Type	3/1	5/2	ν_6 Mars–cross.	ν_6 Earth–cross.
6a	192	S	2.4	0.0	7.6	0.9
6b	192	S	9.5	0.1	25.6	3.8
304	68	C	0.9	0.0	33.2	2.6
623	46	EMPC	18.0	0.0	5.2	0.4
631	60	S	0.3	18.8	1.9	0.6
739	110	EMP	0.0	2.3	35.8	3.5
759	53		1.0	0.3	30.0	8.4
907	66	C	0.4	28.7	1.4	0.6
930	39		3.1	0.0	10.0	1.5
963	11	S	0.1	0.0	14.6	0.7
1222	14		0.0	29.0	19.4	2.5
1468	18		0.1	0.0	99.2	80.0
1892	17		15.1	0.0	2.0	0.4
1916	4	S	0.0	0.0	100.0	13.4
2033	9		0.0	0.0	85.4	3.6
2368	3	SQ	0.1	0.0	99.1	79.3
2548	12		0.7	0.2	31.1	0.8
2604	18		0.4	0.0	72.4	2.4
3402	3		0.0	0.0	97.1	25.8
3833	3		0.0	0.0	96.8	70.9
4095	5		0.0	0.0	47.7	3.3

variables of the planets which are assumed to change with time following the laws provided by the linear theory of Laplace.

In order to study this dynamical system, suitable canonical Arnold action–angle variables (J, ψ, Z, z) are introduced in order to transform K_0 into an Hamiltonian independent of the angles ψ and z. A detailed discussion on these action–angle variables and on the way to handle them numerically can be found in previous papers (Morbidelli 1993; Lemaître & Morbidelli 1993).

The action–angle variables (J, ψ, Z, z) are then introduced in the perturbation K_1, which is expanded numerically in Fourier series of the new angles ψ, z and of time. In these new variables, one proceeds to the elimination of all angular terms in K_1 except the resonant one (providing one is in presence of only one isolated resonance). This is done using the Lie algorithm up to the first order, namely one looks for a generating function W_1 such that

$$\{W_1, K_0\} + K_1 = \text{resonant term} .$$

The generating function W_1 defines new action–angle variables $(\overline{J}, \overline{\psi}, \overline{Z}, \overline{z})$ via the implicit equations

$$\begin{aligned} J &= \overline{J} + \frac{\partial W_1}{\partial \psi}(\overline{J}, \overline{\psi}, \overline{Z}, \overline{z}, t) \\ Z &= \overline{Z} + \frac{\partial W_1}{\partial z}(\overline{J}, \overline{\psi}, \overline{Z}, \overline{z}, t) \\ \psi &= \overline{\psi} - \frac{\partial W_1}{\partial J}(\overline{J}, \overline{\psi}, \overline{Z}, \overline{z}, t) \\ z &= \overline{z} - \frac{\partial W_1}{\partial P}(\overline{J}, \overline{\psi}, \overline{Z}, \overline{z}, t) . \end{aligned} \tag{3}$$

In these new variables, the new Hamiltonian writes (K_0+ resonant term), i.e., in the case of the ν_6 resonance

$$K_0(\overline{J}, \overline{Z}) + \alpha(\overline{J}, \overline{Z}) \cos(\overline{z} + g_6 t + \lambda_6^0) , \tag{4}$$

where g_6 is the average frequency of the longitude of perihelion of Saturn, and λ_6^0 its initial phase. The Hamiltonian (4) is integrable, and is precisely the integrable model of the resonance which is used for the computation of the secular resonant evolution of the orbit.

In order to write (4) in a simpler form, one can introduce new canonical variables:

$$\sigma = \overline{z} + g_6 t + \lambda_6^0 , \qquad S = \overline{Z}$$
$$\theta = \overline{\psi} , \qquad \Theta = \overline{J}$$

so that (4) becomes

$$K_0(S, \Theta) + g_6 S + \alpha(S, \Theta) \cos \sigma . \qquad (5)$$

The dynamics described by (5) is confined on a surface Θ =constant. The values of $\overline{J}, \overline{Z}$ obtained solving Eq. (3) define the value of this constant; moreover $(\overline{J}, \overline{\psi}, \overline{Z}, \overline{z})$ determine also the values of S and σ associated to the present state of the asteroid. These are the initial conditions for the integration of the equations of motion given by (5), which describe the evolution $(S(t), \sigma(t))$ over the time t. Equivalently, one can have a global picture of the resonant phase space by simply plotting the level curves of (5) and putting the present position of the asteroid (S, σ) on this plot.

In conclusion, these are the steps we have followed in this work. For each fictitious fragment, we computed first its mean elements, using the Milani and Kneževič program (Milani & Kneževič 1990), which are the variables associated to the doubly averaged Hamiltonian. Then, we computed its Arnold action–angle variables (J, ψ, Z, z) and, afterwards, its semi–proper variables $(\overline{J}, \overline{\psi}, \overline{Z}, \overline{z})$, by computing the generator W_1 and solving the implicit Eq. (3). The values of $(\overline{J}, \overline{\psi}, \overline{Z}, \overline{z})$ define the value of the constant Θ and the initial condition S, σ for the equations of motion consistent with (5). We integrated these equations in order to find the maximal value of S which corresponds to σ equal to 0 or 180 degrees. The pair (S_{max}, Θ) [i.e. $(\overline{Z}_{max}, \overline{J})$] identifies one orbit of the integrable averaged Hamiltonian K_0, which describes the periodic evolution of the mean values of e and i along with the circulation/libration of the argument of perihelion ω. We chose the reference value $\omega = 90°$ which corresponds to the maximal value of e over the circulation of ω. In this way we finally obtained the peak eccentricity attained by the fictitious fragment during its secular resonant evolution. We considered a fragment as having a Mars– and Earth–crossing orbit when its perihelion distance became less than 1.703 and 1.058 AU, respectively, since according to the numerical integration of Quinn et al. (1991, Table I) these values represent the maximum aphelion distances reached by Mars and the Earth over a time span of 3 Myr. Of course this criterion is not rigorous, but for our purposes it represents a reasonable approximation.

We also wanted to count how many fragments from each parent asteroid were dropped into the 3/1 and 5/2 mean motion resonances with Jupiter, which are also likely to give raise to a chaotic evolution leading to Earth–crossing. A fragment was considered as injected in the chaotic zone associated with the 3/1 resonance whenever its mean semimajor axis and eccentricity were such that

$$(2.497 - e/8.850) \text{ AU } < a < (2.510 + e/9.615) \text{ AU} ,$$

in agreement with the results of numerical experiments on the dynamics of this resonance and the observed width of the corresponding Kirkwood gap (Yoshikawa 1990, Fig. 2). A similar criterion for the 5/2 resonance is

$$2.815 \text{ AU} < a < 2.830 \text{ AU}$$

for $e < 0.15$ and

$$[2.815 - 0.1(e - 0.15)] \text{ AU} < a < [2.830 + 0.15(e - 0.15)] \text{ AU}$$

for $e > 0.15$ (Yoshikawa 1991, Fig. 16).

4. Results

The asteroids included in our sample have been chosen according to the following criteria: either they had been estimated by Farinella et al. (1993a, Table 1) to inject more than 30% of their fragments in a strip of width 1 arcsec/yr in the g frequency about the resonance surface $g = g_6$ (asteroids 6, 304, 623, 631, 759, 907, 930, 1468, 1892, 2368, 2548, 2604, 3402), or they were included in the list of asteroids so close to the resonance that their non–resonant proper elements could not be computed accurately (Lemaître & Morbidelli 1993; Morbidelli 1993; asteroids 6, 623, 739, 759, 930, 1222, 1468, 1892, 1916, 2033, 2368, 2548, 2604, 3402, 3833, 4095). Of course, the two lists overlap to a considerable extent. The sample includes the two asteroids which were already known to be librating inside the resonance, 759 Vinifera and 1222 Tina (Froeschlé & Scholl 1987), and three bodies which according to Morbidelli (1993) are expected to get their eccentricities pumped up to > 0.6 by the resonance (1468 Zomba, 2368 Beltrovata, and 3833 1971 SC). Figure 1 shows the position of these bodies in the mean inclination vs. semimajor axis plane; the dashed region corresponds to the initial conditions for which, with a mean eccentricity of 0.15, Morbidelli's theory predicts a maximum eccentricity > 0.4. The diagram is repeated four times according to different combinations of the angular elements relevant for the location of the secular resonance, and each asteroid is plotted in the diagram corresponding to the closest choice of mean ω and Ω. Note, though, that this provides only an approximate view of the position of the asteroids with respect to the "dangerous" strip, because changing e, ω and Ω would somewhat shift the location of the latter.

Our 20 asteroids can also be grouped in three categories according to their current orbital elements, as listed in Table 1: (1) those lying near the inner boundary of the main belt, with semimajor axes < 2.3 AU (963, 1468, 1916, 2033, 2368, 3402, 3833, 4095); (2) those with semimajor axes close to 2.4 AU and inclination near 14° (6, 304, 623, 930, 1892, 2604); (3) those with semimajor axes between 2.6 and 2.8 AU and inclinations of about 20° (631, 739, 759, 907, 1222, 2548). Actually, these are the three regions where the ν_6 resonance had been predicted to be a potentially efficient collector of planet–crossing fragments, as explained in Sect. 1.

Coming to the results of our calculations, for each of the 20 asteroids listed in Table 1, in Table 2 we have listed the diameter (derived according to the procedure described in Cellino et

Table 3. For each of the 20 asteroids listed in Table 1, the Table gives the percentage of the total Earth impact yield through ν_6 (E_1) and through both ν_6 and 3/1 (E_2). The Earth impact yield has been obtained by multiplying the percentages listed in Table 2 times a scaling factor depending on the asteroid's size (see text)

No.	E_1	E_2
6	26.03	48.7
304	8.21	5.35
623	0.48	10.6
631	1.39	1.01
739	36.8	17.8
759	14.2	7.71
907	1.76	1.42
930	1.18	1.75
963	0.02	0.01
1222	0.15	0.07
1468	9.11	4.42
1892	0.04	0.74
1916	0.04	0.02
2033	0.07	0.04
2368	0.10	0.05
2548	0.03	0.03
2604	0.27	0.16
3402	0.03	0.02
3833	0.09	0.04
4095	0.02	0.01

al. 1991), the taxonomic type (Tholen 1989) and the percentages of fragments dropped in the 3/1 and 5/2 Kirkwood gaps and achieving Mars– or Earth–crossing orbits due to ν_6 resonant perturbations, according to the criteria described in Sect. 2. Asteroid 6 Hebe appears twice, as we tested the behavior of fragments ejected from it both with V_{min} = 100 m/s (6a) and with V_{min} = 200 m/s (6b).

The asteroids which inject in ν_6 the highest fraction of Earth–crossing fragments are of course those which become Earth–crossers themselves (1468, 2368, 3833), albeit not — in the cases of 2368 and 3833 — during the limited time span of our integrations. Potentially efficient meteorite deliverers are also 1916 and 3402: the former has a fairly large eccentricity at the beginning of the integration, the latter starts from a semi-major axis of 2.13 AU, very close to the inner boundary of the main asteroid belt (see Scholl & Froeschlé 1991).

However, it is important to recall that large asteroids produce a more intense fragment flux as a consequence of their higher cross–section and mass. Farinella et al. (1993a) have estimated that for radii $R < R_{min} = 83\,\mathrm{km}\,(V_{min}/100\,m/s)$ the mass ejection rate of an asteroid is proportional to $R^{(5-b)}$, where b is the projectile size distribution index, typically in the range from 2 to 2.5; for large bodies such as Hebe, for which $R > R_{min}$ (i.e., the gravitational reaccumulation of part of the ejected fragments must be accounted for), the above scaling factor becomes $R^{(5-b)}(R/R_{min})^{(1-\alpha)}$. Thus, using the radii listed in Table 2 and assuming b = 2.5, we have transformed the percentages of fragments injected into Earth–crossing orbits into *Earth impact yields*, which should be roughly proportional to the mass influx onto the Earth from each asteroid (see Table 3). From Table 3, where the total Earth impact yield from the 20 asteroids has been normalized to 100, one can estimate that Hebe's 3.3% of Earth–crossing fragments — summing up those injected in the ν_6 and 3/1 resonances for V_{min} = 100 m/s — corresponds to an Earth impact yield 6.3 times larger than that corresponding to the 9.4% of 759 Vinifera, 11.0 times that of 1468 Zomba (80.1%) and about 980 times that of 2368 Beltrovata (79.4%). The meteorite yield of Hebe increases by about 4 times for V_{min} = 200 m/s. We recall that in Farinella et al. (1993a,b) we assumed that 10% of the fragments from Hebe end up into Earth–crossing orbits, and from this we estimated that the absolute meteorite flux to be expected from Hebe is of the order of 10% of the observed influx.

Another important remark is that, on a time scale of the order of 10^8 Myr, it is also likely that many Mars–crossing (or even Mars–grazing) fragments will end up into Earth–crossing orbits, as a consequence of repeated Mars encounters, changing their location in a random–walk fashion with respect to the resonance (Wetherill & Williams 1979). While this indirect mechanism involves a much longer time for transport of fragments into Earth–crossing orbits, its efficiency with respect to direct resonant transport is increased by the fact that, as shown in Table 2, most asteroids produce a much larger proportion of Mars–crossers than of Earth–crossers. However, a quantitative assessment of this mechanism requires a different type of algorithm, capable of accounting for the effects of close encounters between an asteroid and a planet (see Wetherill 1985, 1987).

Some more comments can be done by inspecting in more detail the individual dynamical behavior of the asteroids. Figures from 2 to 15 refer to some of the cases we have studied. Each figure is composed of 6 pictures. In them all, the abscissa gives the fragment serial number; since, as explained in Sect. 2, the fictitious fragments are ejected at random epochs during the integration interval (in bursts of 10 at a time), this serial number is roughly proportional to the ejection time since the beginning of the integration. The first 4 pictures show the semi–proper elements of the fragments. As discussed in section 3, these are the orbital parameters after elimination of the short periodic and non–resonant secular terms. This is the reason why, as one can appreciate by eye, the eccentricity and inclination are filtered of all oscillations, and therefore show only the secular trend, correlated with the distribution of the critical angle of the

ν_6 resonance, called σ. This secular trend recalls the evolution with time of the semi–proper elements of the parent body. Note that the inclination has a minimum when the eccentricity has a maximum.

The last two pictures show the resonant proper elements of the fragments, i.e. the maximal eccentricity and the minimal perihelion distance during their secular evolution in the ν_6 resonance. Fragments which become Mars– and Earth–crossers are indicated by triangles and asterisks, respectively (the study of the fragment orbits has been stopped when q became < 1 AU, so these bodies lie aligned near the top and the bottom of the diagrams showing e_{max} and q_{min}, respectively). Note that in the picture showing e_{max} most fragments have the same value, and this value corresponds to the maximal semi–proper eccentricity of the distribution shown in the second picture. This gives a hint on the correctness of resonant proper elements and on their consistency with the numerical integration of the parent body.

Figures 2 and 3 refer to the fragments ejected from 6 Hebe, assuming V_{min} equal either to 100 or to 200 m/s. It can be noted that 6 Hebe, as several analyzed bodies, is a more efficient deliverer of planet–crossing fragments when e is close to the minimum of its secular cycle; possibly this can be explained by the fact that, when e is small, the dispersion of the fragments is larger, especially in σ. Also, the fragments which are most likely to reach small perihelion distances are those starting from semimajor axes somewhat smaller than that of Hebe itself, in agreement with the results of Farinella's et al. (1993b) numerical experiments. This is due to the fact that one needs to increase the inclination of Hebe by about 4 degrees in order to enter the dangerous regions of the resonance (i.e. the regions which pump the eccentricity up to planet–crossing values), and similar changes in i are not possible with the ejection velocities of our experiments. Therefore, the only fragments which can fall in the dangerous regions are those who have a smaller semimajor axis, where the ν_6 resonance comes down at lower inclination.

The relatively simple behavior of 6 Hebe has a close analogue for most of the other asteroids lying in the same zone (for example 623 Chimaera and 1892 Lucienne, which are efficient fragment deliverers also to the 3/1 gap). Figures 4, 5 and 6 show what happens in the cases of 2604 Marshak, 930 Westphalia and 304 Olga. All of them are more efficient fragment deliverers than Hebe. 2604 Marshak, whose starting orbit is similar to Hebe's but with a somewhat lower semimajor axis, just puts more fragments in the a range where the eccentricity is most easily pumped up. 930 Westphalia, whose starting inclination is some 2° higher than Hebe's, just librates in the resonance with a fairly small amplitude, like in the well known case of 759 Vinifera (to our knowledge, this is the first asteroid discovered to librate in ν_6 with a semimajor axis smaller than that corresponding to the 3/1 gap); most of Westphalia's fragments just behave like their parent body, and do not become planet–crossers. For what concerns 304 Olga our statistics is not complete; since Olga passes through $e = 0$ (where our action–angle variables are singular), the algorithm for the computation of semi–proper elements does not converge for those fragments with very small eccentricity, i.e. about from No. 100 to 250.

The asteroids lying close to the inner boundary of the belt are in general fairly efficient deliverers of planet–crossing fragments; some of them are indeed currently Mars–crossers or Mars–grazers. Their behaviors range from the relatively simple ones of 963 Iduberga and 2033 Basilea (see Figs. 7 and 8), which just circulate and again inject most of the small–perihelion fragments near the minimum of their eccentricity cycles, to the more complex patterns of 3833 1971 SC (Fig. 9), 3402 Wisdom (Fig. 10), 1916 Boreas (Fig. 11), 1468 Zomba (Fig. 12) and 2368 Beltrovata (Fig. 13). The dynamics of the two latter asteroids, who themselves become Earth–crossers, is discussed in Morbidelli (1993); of course, most of their fragments share their fate.

Among the asteroids residing between the 3/1 and 5/2 gaps, we have two different behaviors: the librators, like 759 Vinifera (Fig. 14) and 1222 Tina, which inject a significant fraction of fragments into orbits reaching the inner planets; and the circulators, like 631 Philippina, 907 Rhoda, 739 Mandeville (Fig. 15; see also Fig. 4 in Morbidelli 1993), and 2548 Leloir (Fig. 16), which are much less efficient in injecting fragments into the ν_6 resonance. This fact is explainable as follows. In this part of the belt, the ν_6 resonance is located at a constant inclination, independent of the semimajor axis. Therefore, the mechanism for injecting fragments in the dangerous regions of the ν_6 resonance is to give them a sufficiently large Δi, instead of a sufficiently large Δa as it is the case in the inner belt. In Fig. 14, concerning Vinifera, it is evident that the Mars– and Earth–crossing fragments are those which have the largest semi–proper inclination, regardless of their semimajor axis. The same happens for 1222 Tina. Both these asteroids, being ν_6 librators, are close enough to the dangerous region of the secular resonance to be able to inject many fragments via the Δi mechanism. Conversely, the circulators as Philippina, Mandeville etc. are too far from the resonance to be able to inject in it a significant fraction of fragments. Note moreover that some of these bodies (631, 907, 1222) inject substantial fractions of their fragments in the 5/2 resonance, rather than in ν_6; these fragments are also likely to become Earth–crossers, as shown by the existence of several Apollo objects lying currently in the 5/2 chaotic zone (Hahn et al. 1991).

The algorithm described in Sect. 3 also allows us to estimate the time needed for the fragments to reach the Earth–crossing state starting from the ejection epoch. Figures 17 and 18 show histograms for the number of fragments (over the 10^3 ejected) delivered by asteroids 1468 and 3833 which achieve Earth–crossing orbits after a given time t. This time is typically of the order of 0.5 to 1 Myr, with a tail reaching 2 Myr. It is anyway much shorter than the time required for having the orbits influenced in a significant way by Mars encounters ($\approx 10^8$ yr); we recall that the typical lifetime of an Earth–crossing body vs. collision with the Earth is also of the order of 10^8 yr.

5. Conclusions

This work has consisted in coupling Morbidelli's (1993) theory for the dynamics of ν_6–resonant orbits and Farinella's et al. (1993a) model for the collisional ejection of fragments from

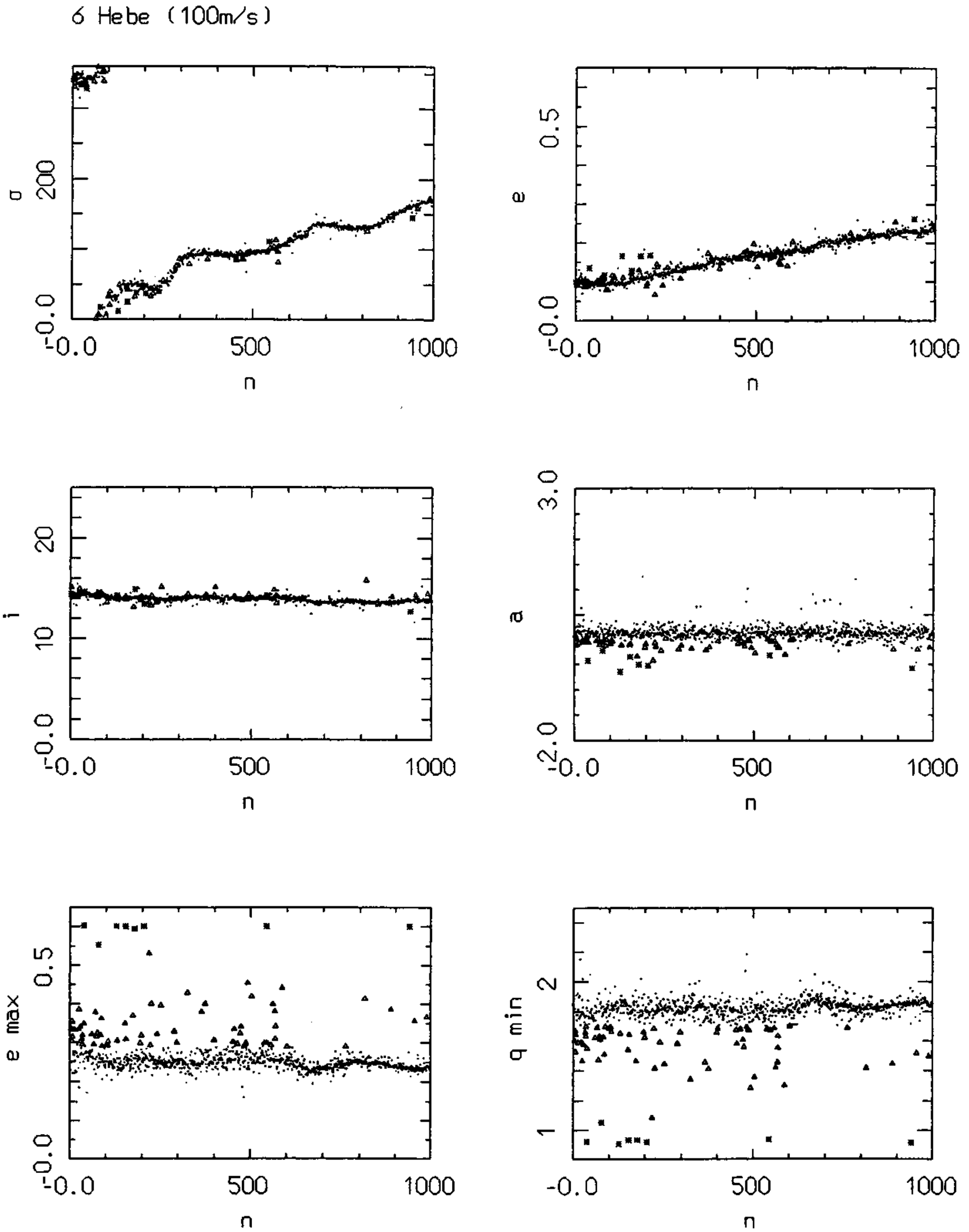

Fig. 2. a, e, i, σ, the maximum eccentricity e_{max} and the minimum perihelion distance q_{min} vs. the fragment serial number (roughly proportional to ejection time) for all the fragments ejected from 6 Hebe, assuming V_{min} = 100 m/s. Triangles and asterisks indicate Mars– and Earth–crossers, respectively

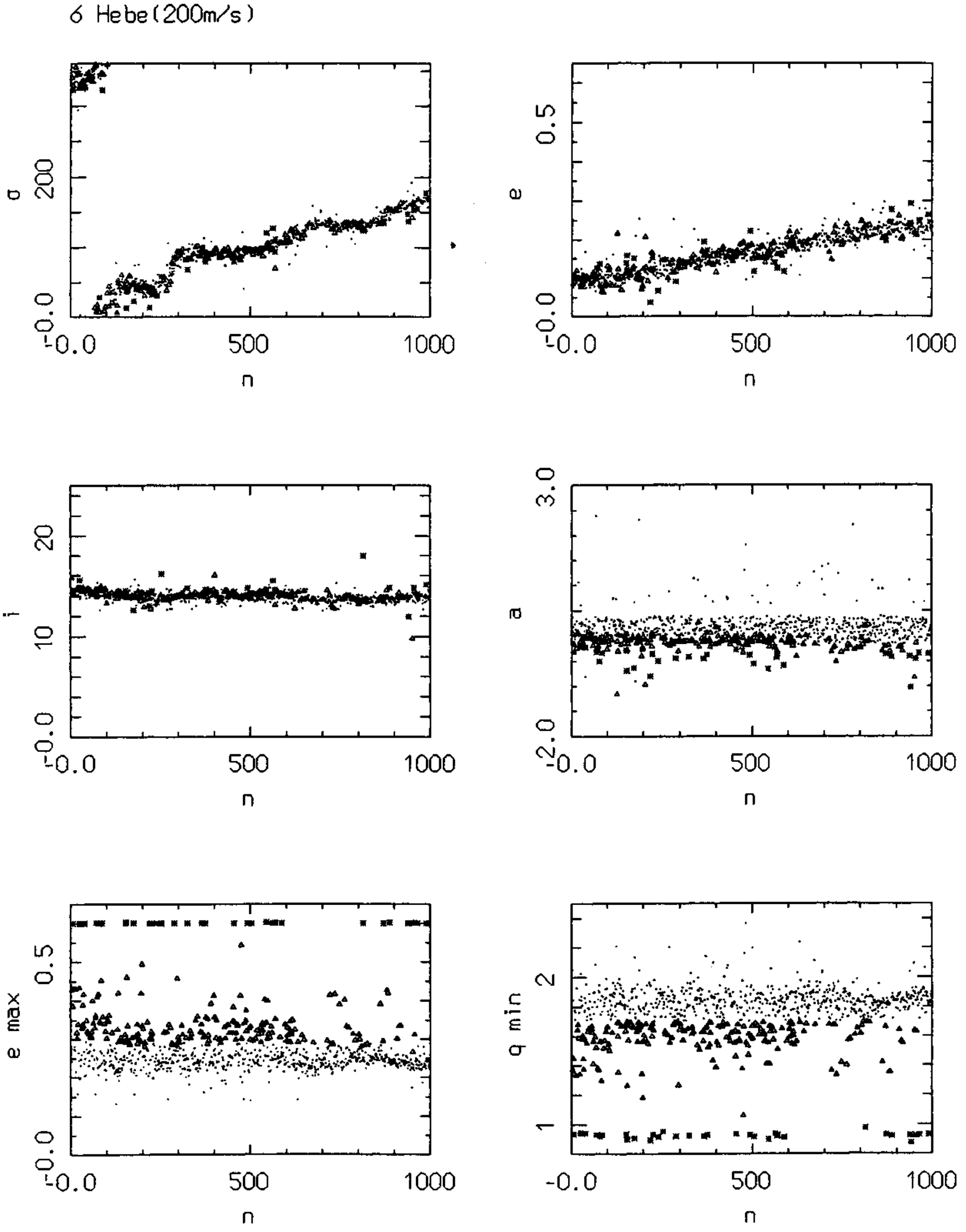

Fig. 3. The same as Fig. 2, but for V_{min} = 200 m/s

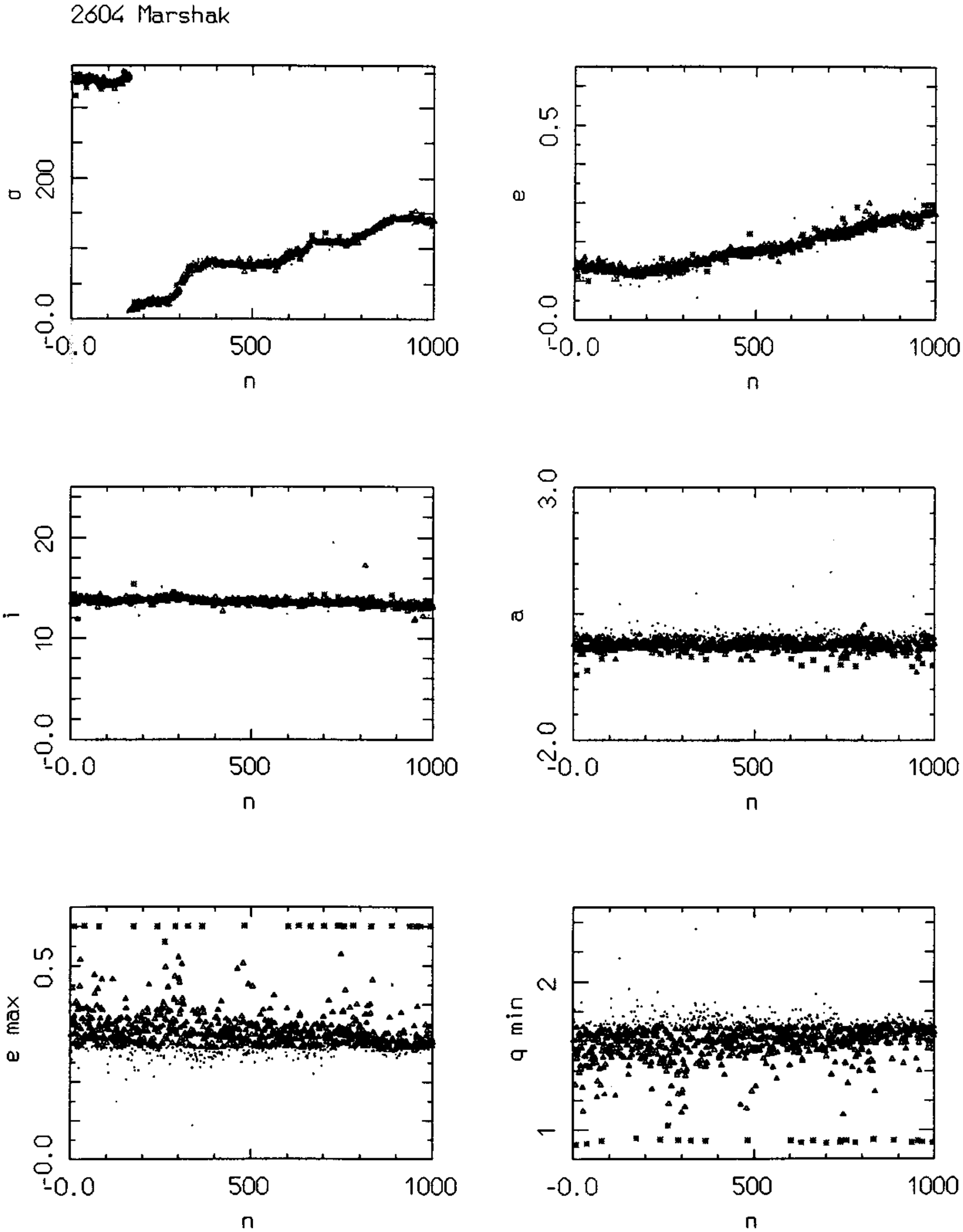

Fig. 4. The same as Fig. 2, but for 2604 Marshak

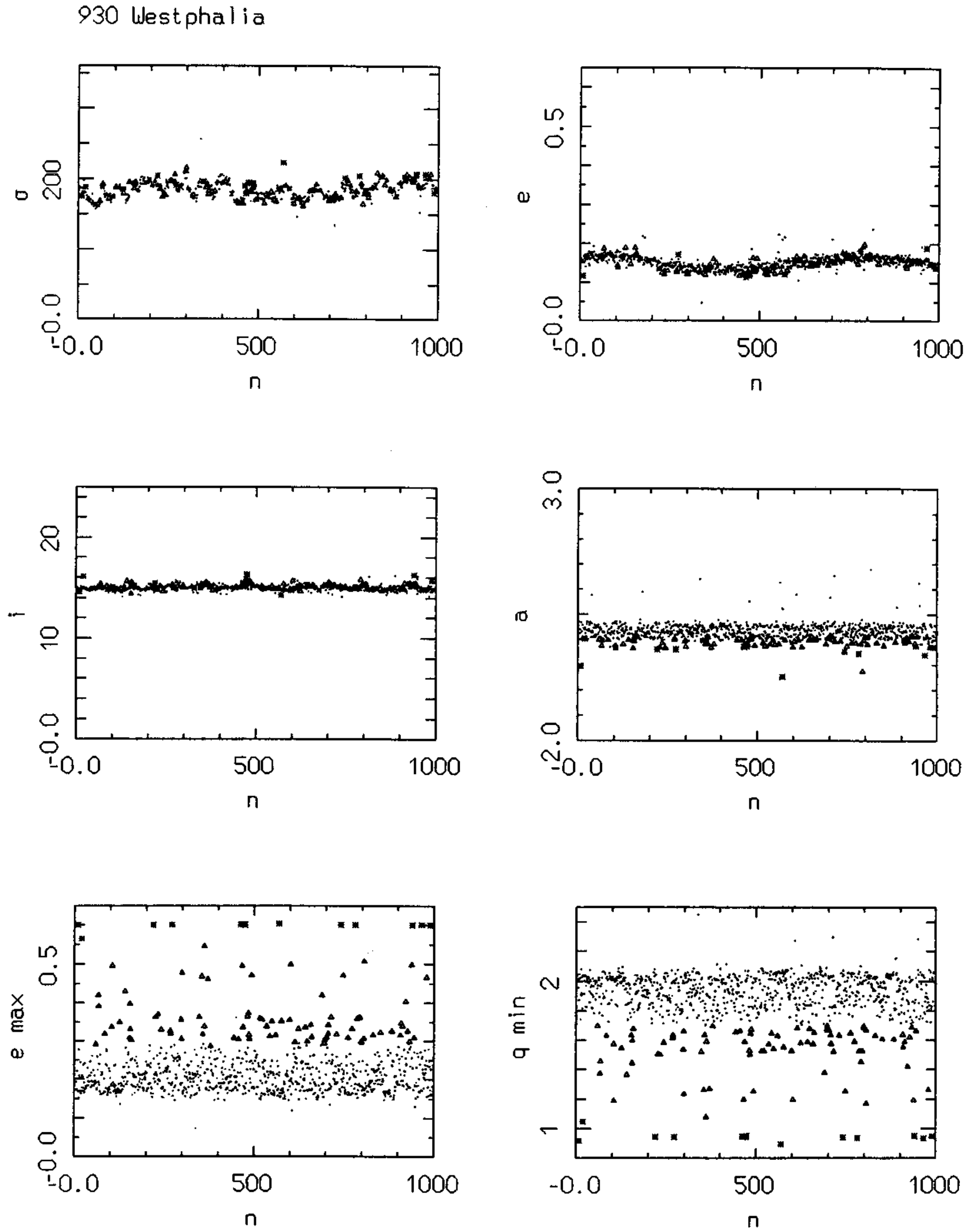

Fig. 5. The same as Fig. 2, but for 930 Westphalia

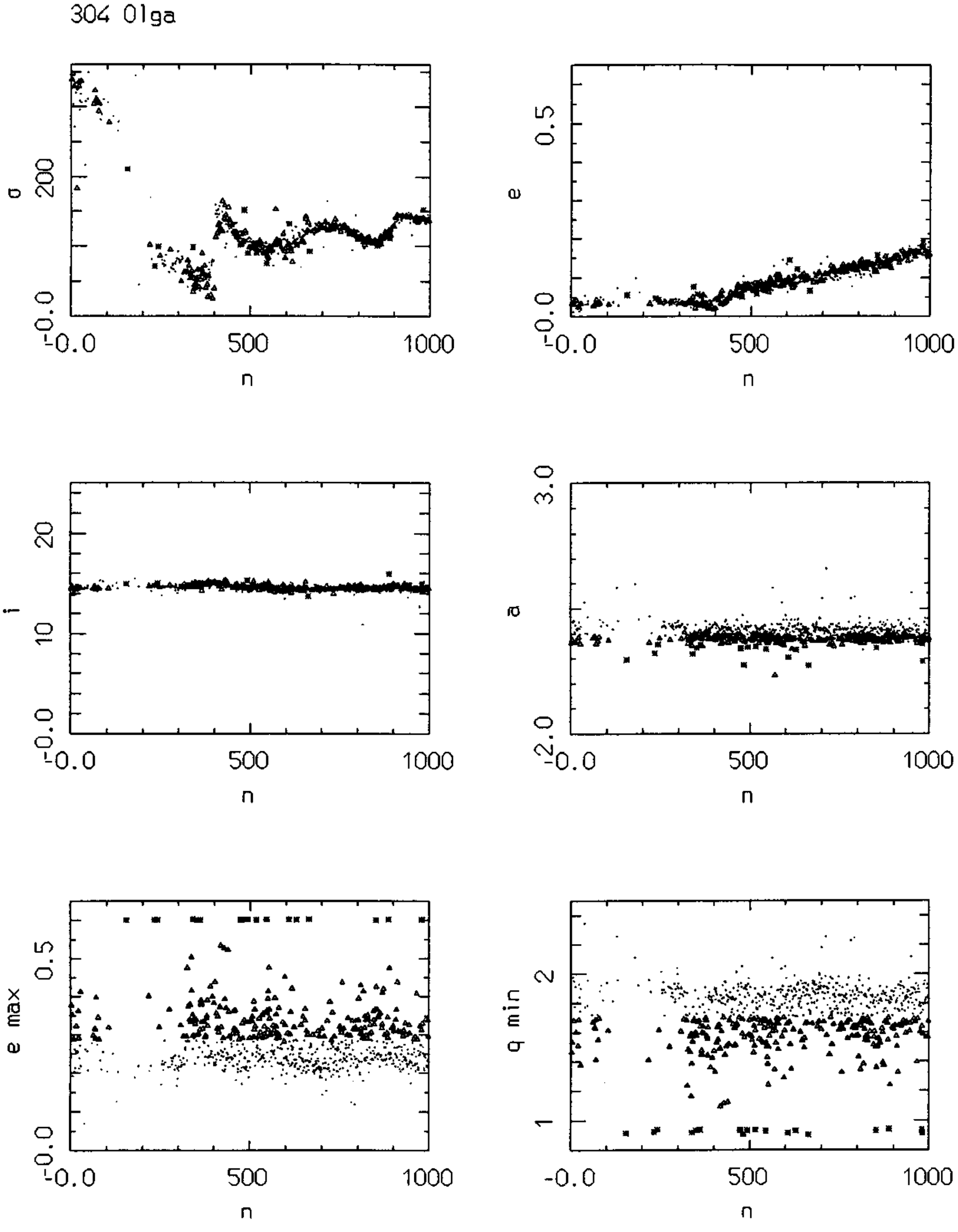

Fig. 6. The same as Fig. 2, but for 304 Olga

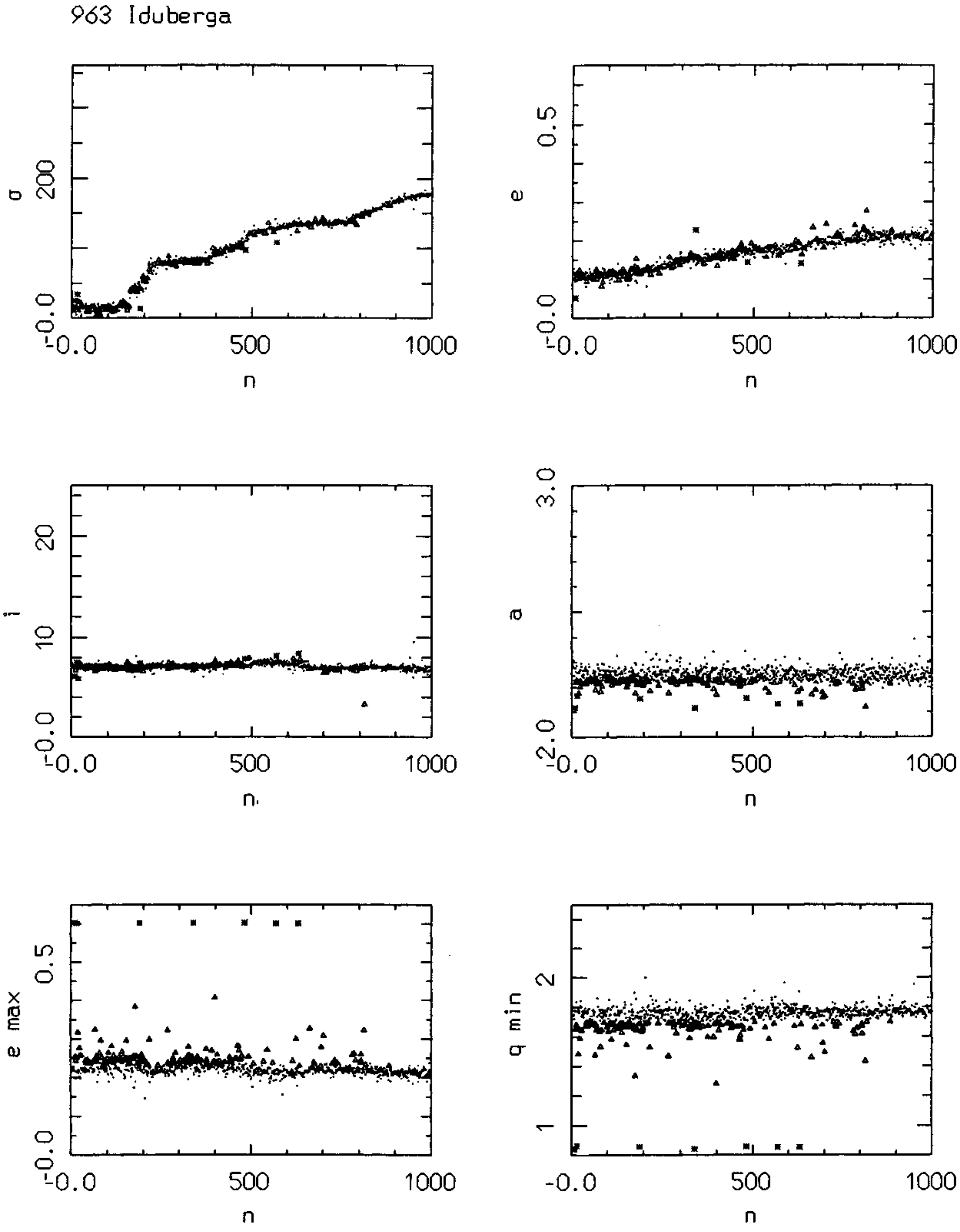

Fig. 7. The same as Fig. 2, but for 963 Iduberga

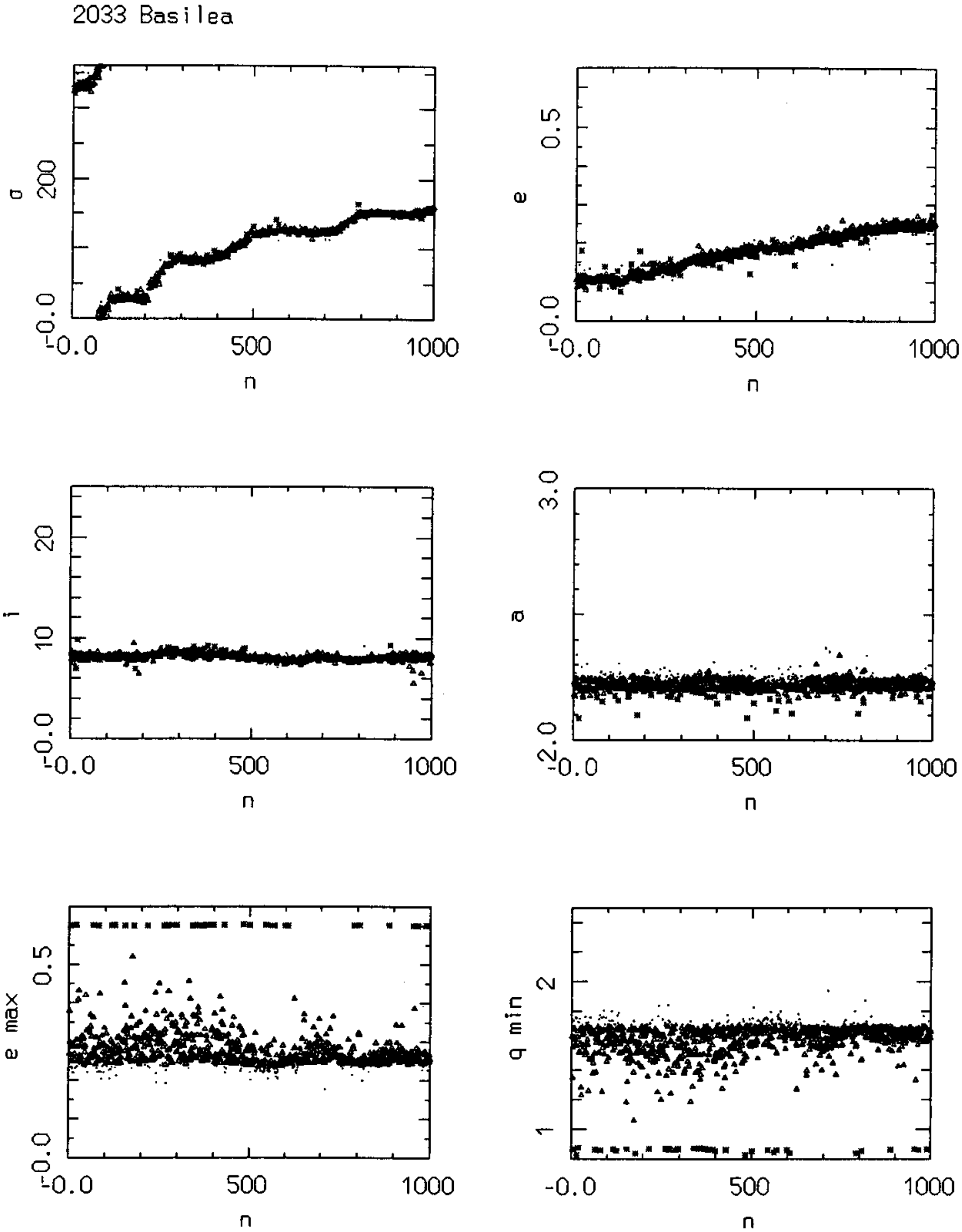

Fig. 8. The same as Fig. 2, but for 2033 Basilea

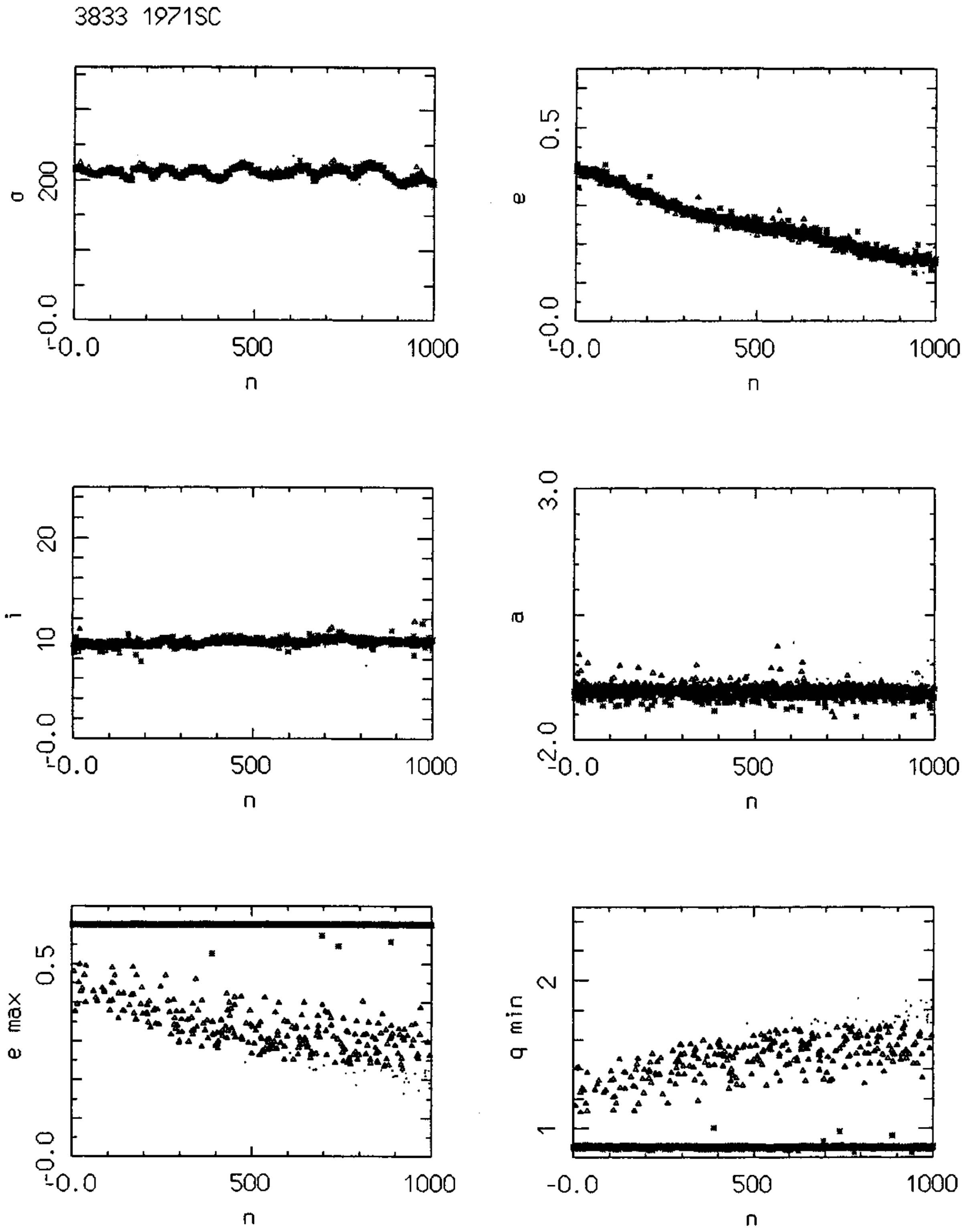

Fig. 9. The same as Fig. 2, but for 3833 1971 SC

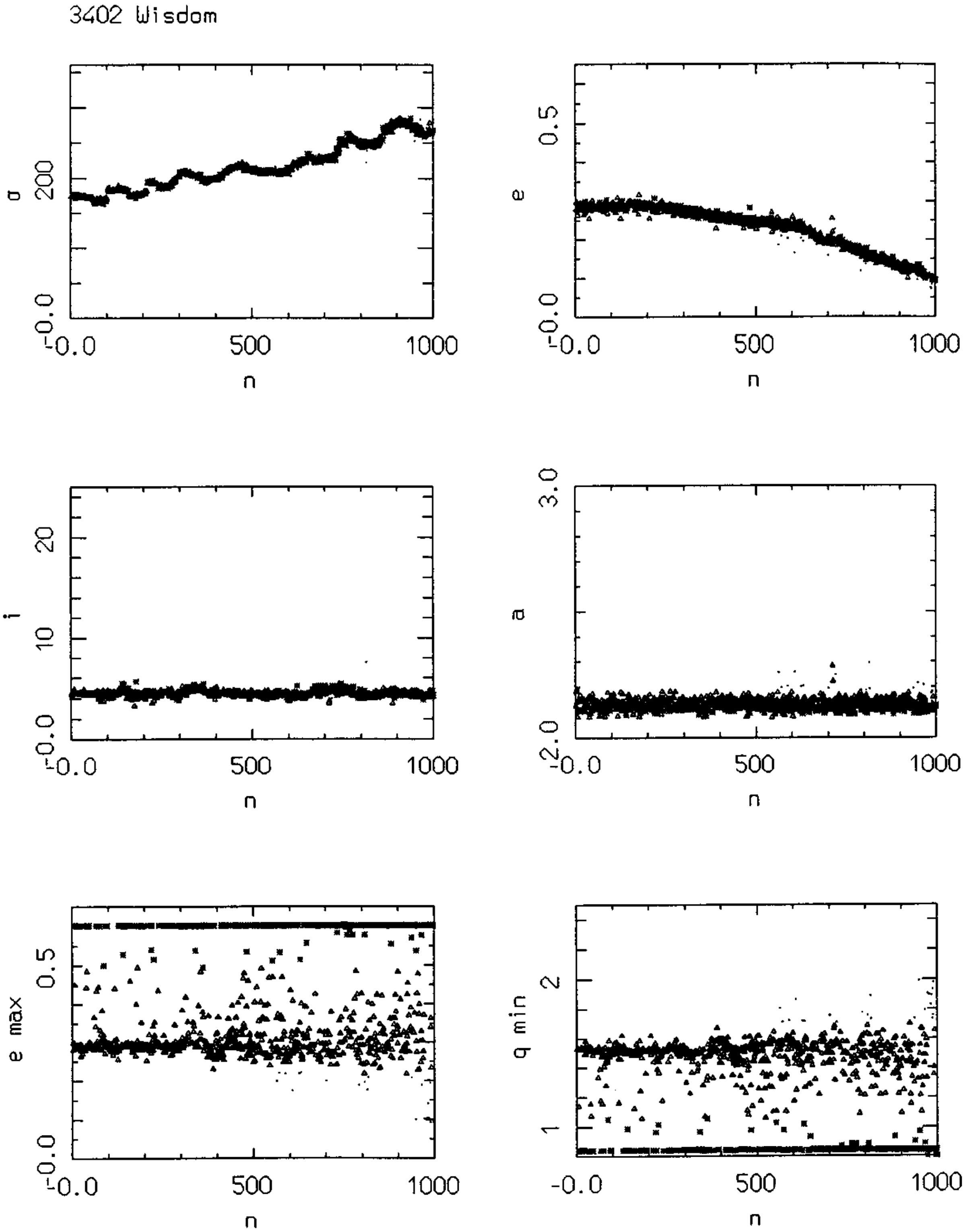

Fig. 10. The same as Fig. 2, but for 3402 Wisdom

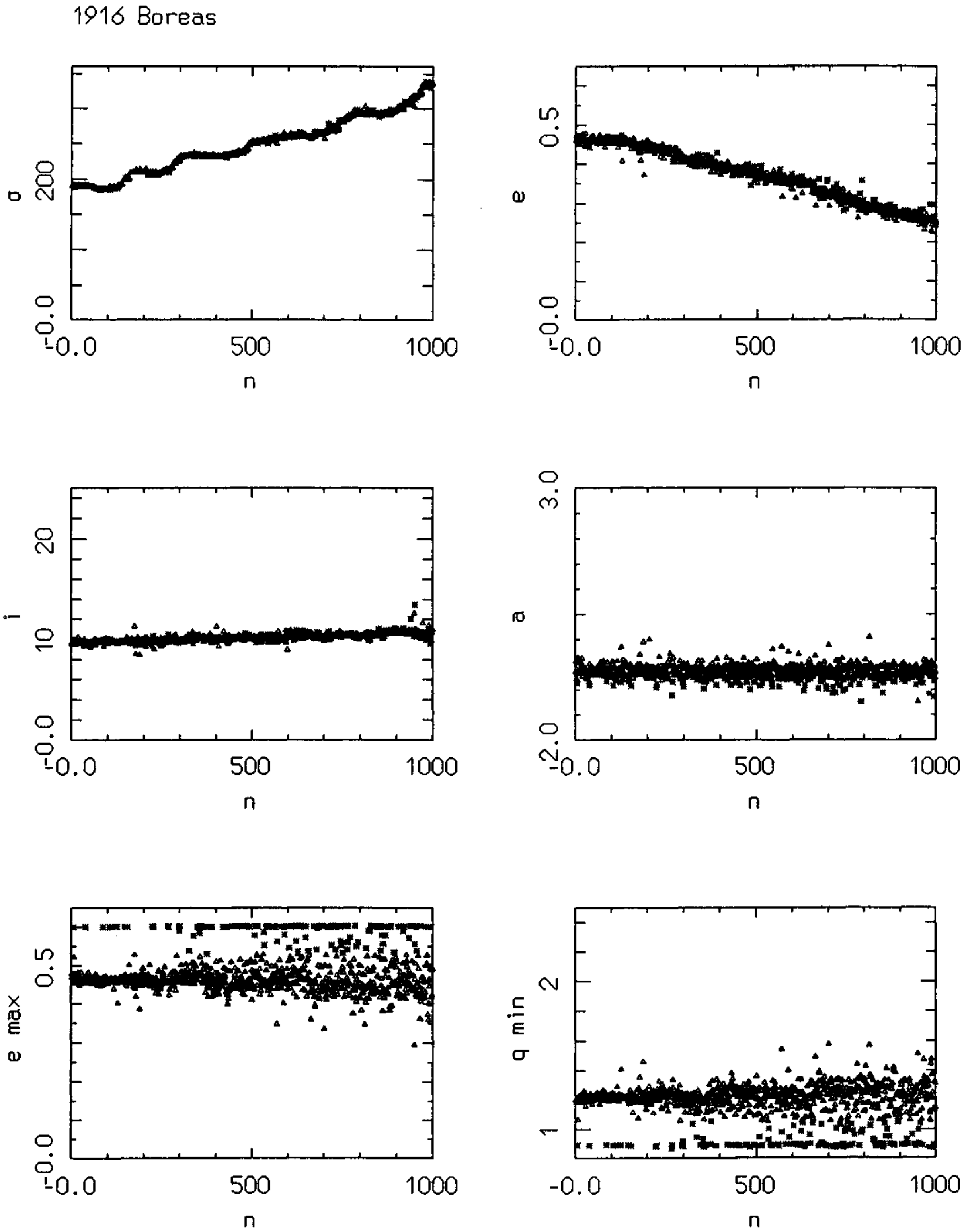

Fig. 11. The same as Fig. 2, but for 1916 Boreas

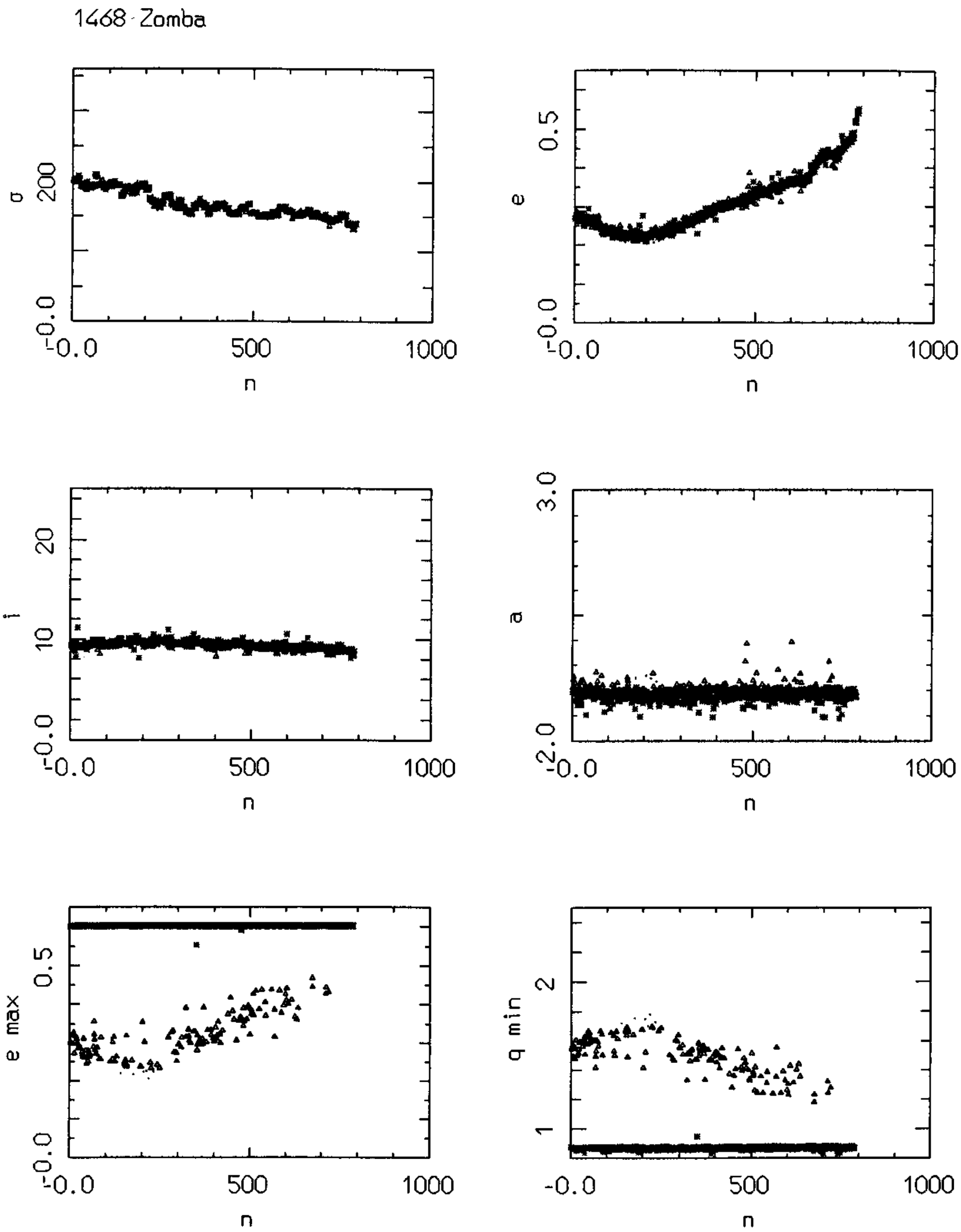

Fig. 12. The same as Fig. 2, but for 1468 Zomba

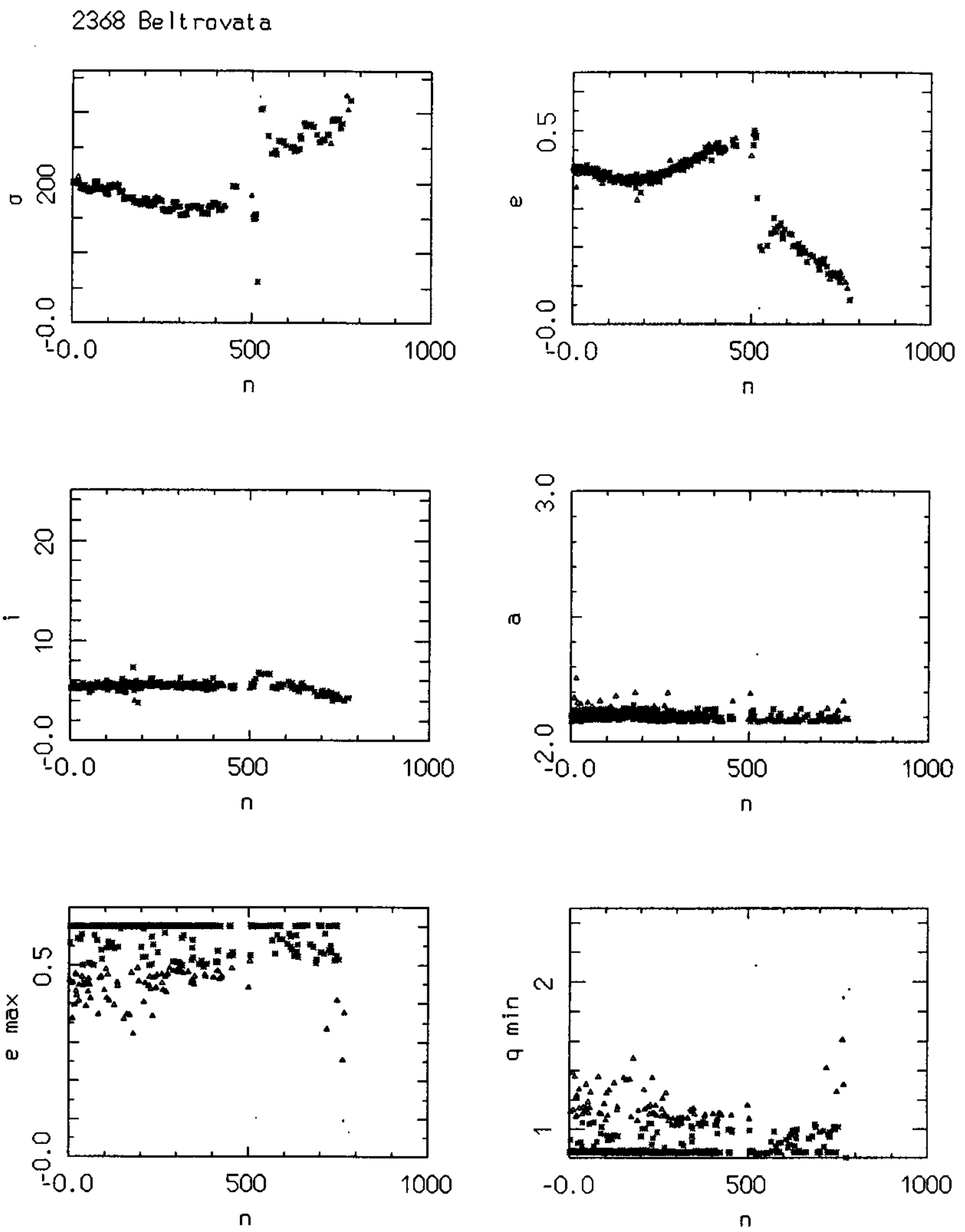

Fig. 13. The same as Fig. 2, but for 2368 Beltrovata

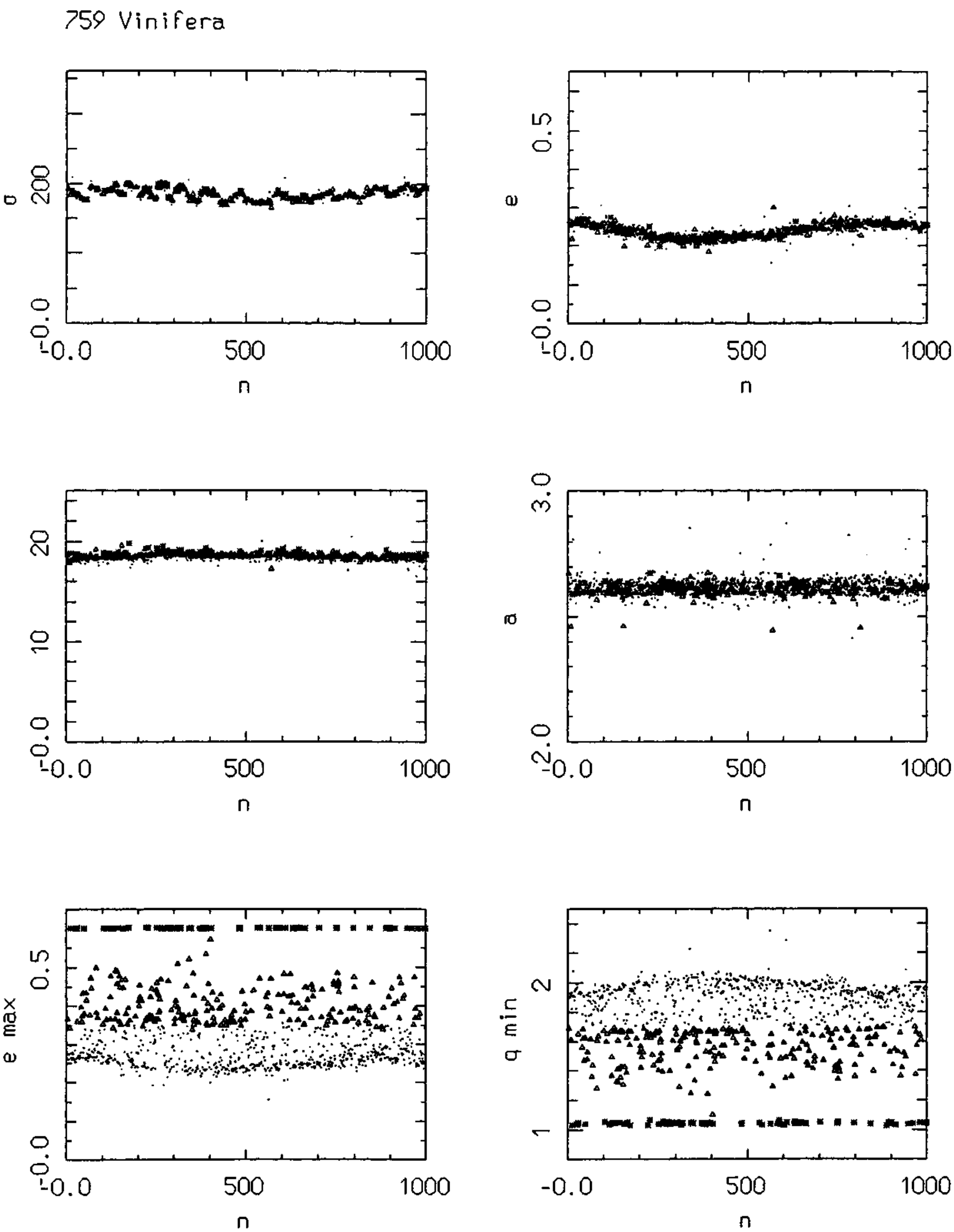

Fig. 14. The same as Fig. 2, but for 759 Vinifera

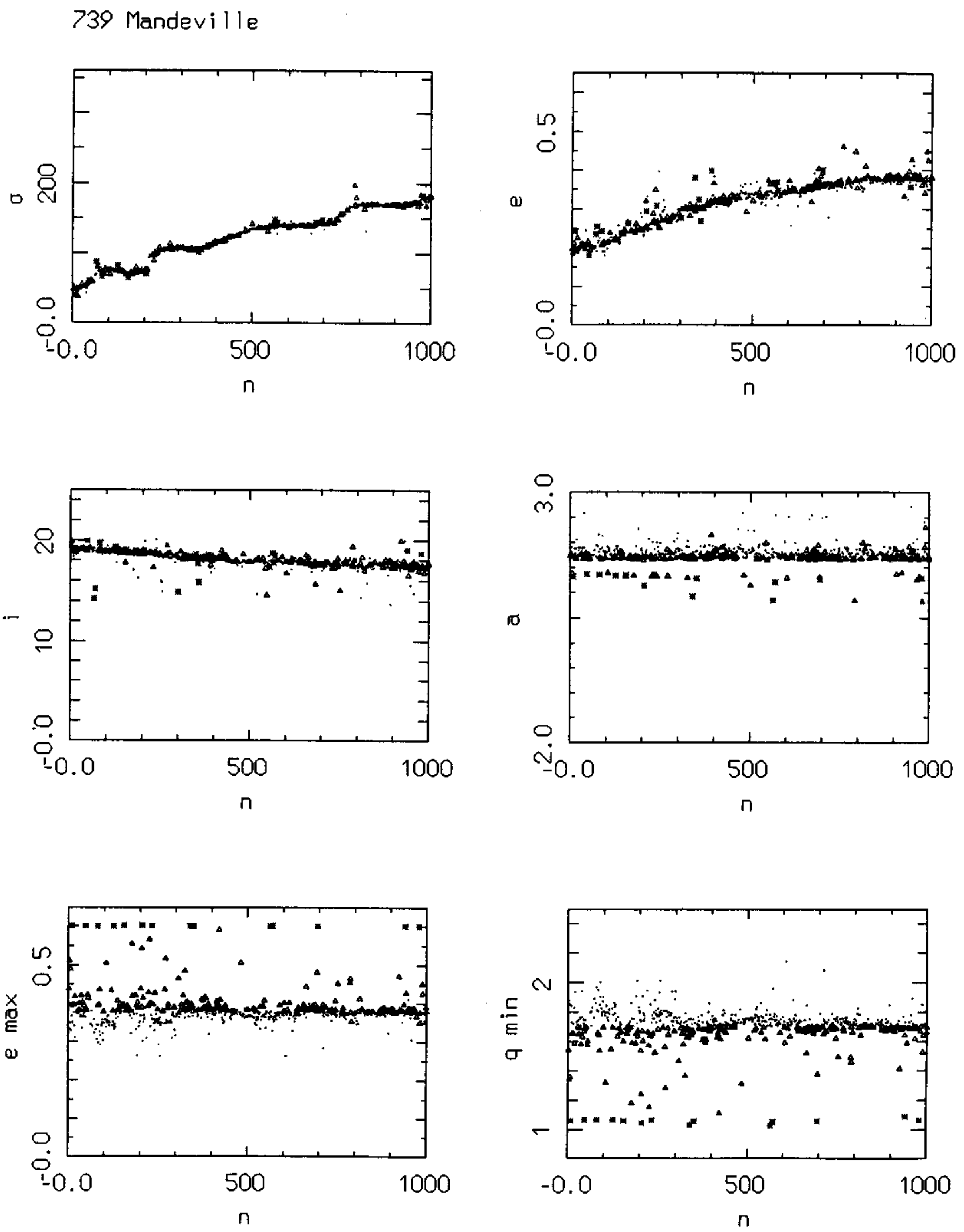

Fig. 15. The same as Fig. 2, but for 739 Mandeville

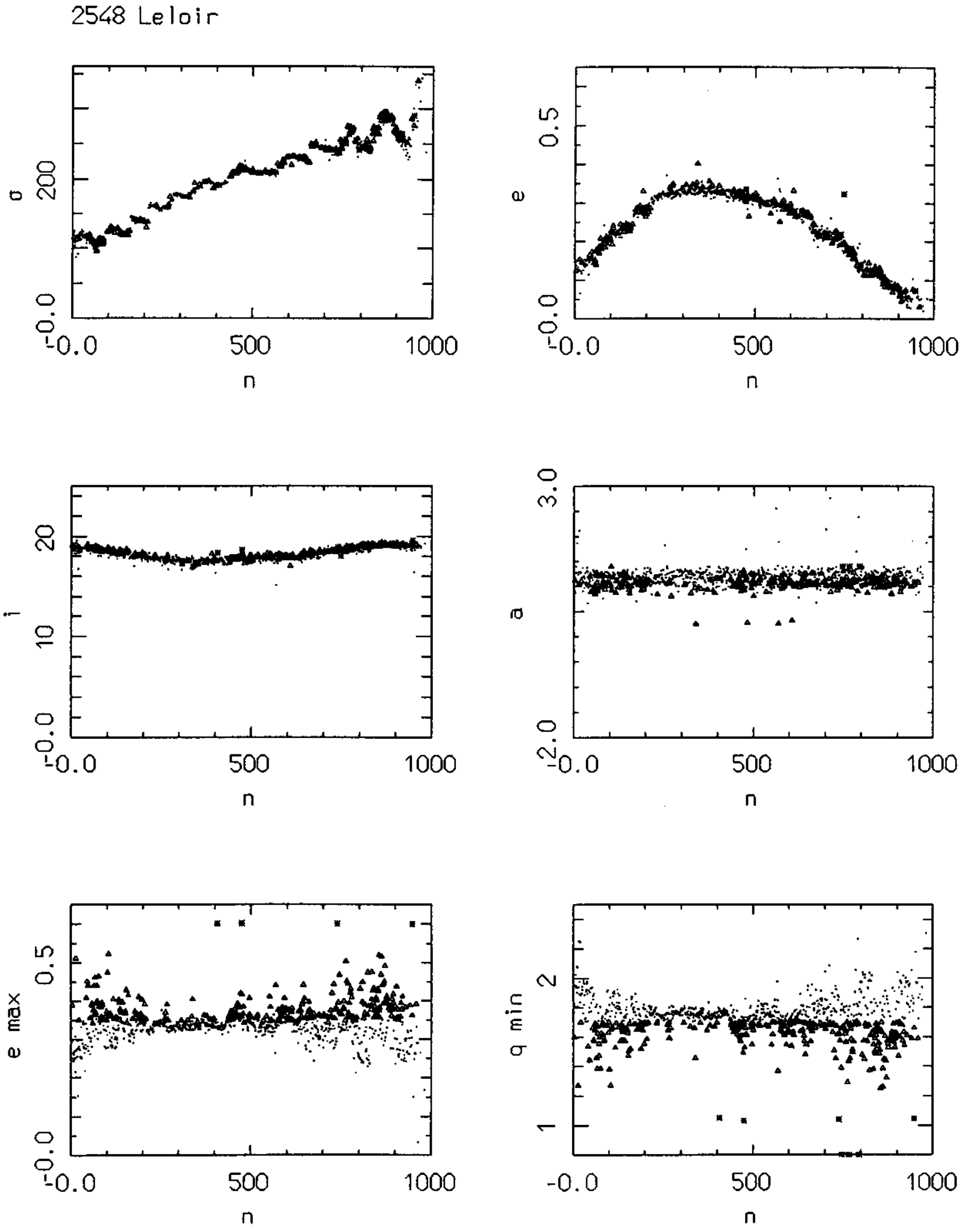

Fig. 16. The same as Fig. 2, but for 2548 Leloir

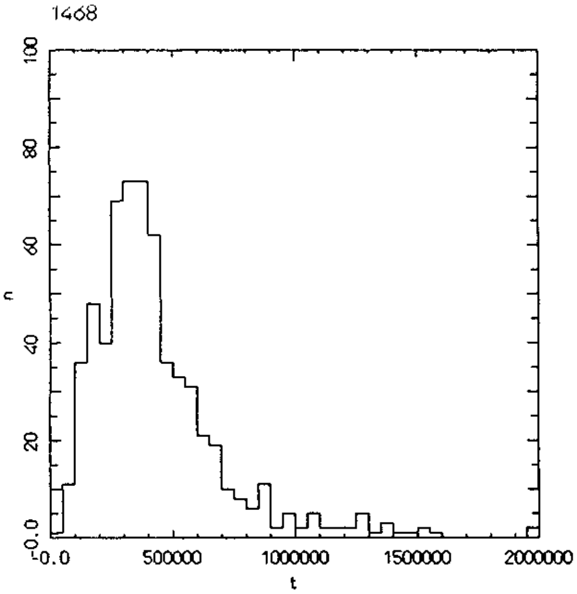

Fig. 17. Histogram of the times, starting from the ejection epoch, at which the fragment ejected from 1468 Zomba achieve Earth–crossing orbits

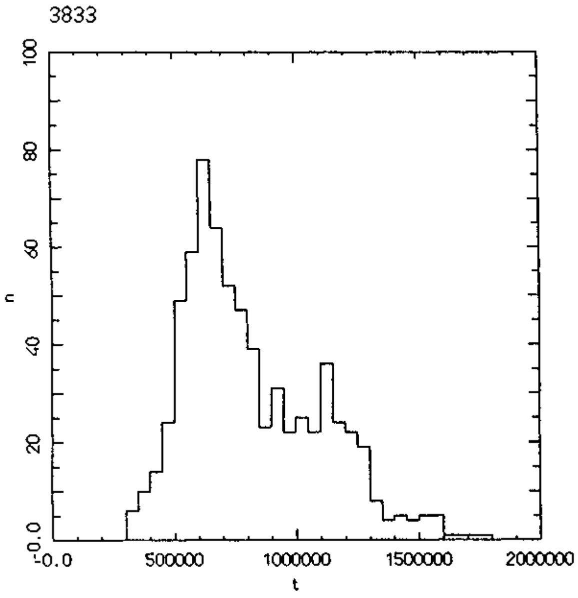

Fig. 18. The same as Fig. 17, but for 3833 1981SC

existing main–belt asteroids. In this way we have been able to estimate the efficiency of 20 asteroids close to the ν_6 resonance as potential deliverers of planet–crossing fragments — that is, in the case of Earth, of meteorites. We have found that several of these asteroids do inject into the resonance a significant fraction of their fragments, which then have their orbital eccentricities increased up to Mars– and even Earth–crossing values. We conclude that some of these bodies — in particular the largest ones, like 6 Hebe, 304 Olga, 739 Mandeville and 759 Vinifera — are probably efficient deliverers of meteorites. The time required for the fragments to be transported into Earth–crossing orbits is typically of the order of 10^6 yr for those bodies whose eccentricity is pumped up by the resonance to ≈ 0.6, whereas it is some 100 times longer when Mars encounters are needed as an intermediate process. Other asteroids inject a substantial fraction of their fragments into the gaps corresponding to the 3/1 (623 Chimaera, 1892 Lucienne) and 5/2 (631 Philippina, 907 Rhoda, 1222 Tina) mean motion resonances.

From Table 2 it is apparent that only for a fraction of our sample asteroids — typically, the largest ones — reliable taxonomic classifications are available. We suggest that all these asteroids should become high–priority targets for new, detailed spectrophotometric investigations at visual and infrared wavelengths, in order to determine their taxonomic types and to assess their similarity to some of the known meteorite types. While this research area has recently seen a burst of activity (see e.g. Vilas & McFadden 1992; Britt et al. 1992; Burbine et al. 1992; Gaffey et al. 1993), we believe that still much remains to be done. We stress that following this and our previous studies, it appears likely that a large fraction of all meteorites and near–Earth asteroids are delivered by a small and possibly nonrepresentative sample of the known main–belt asteroid population, consisting of relatively large bodies located in the vicinity of resonances.

In the next stage of our research project, we plan to develop a realistic model for the dynamical evolution of planet–crossing objects generated in the asteroid belt, taking into account resonances, close encounters and collisions both with other asteroids and with the planets themselves. The final aim is that of predicting the orbital and size distribution, the time variability, the lifetimes and the compositions of the NEA/meteoroid population.

Acknowledgements. P.F. carried out this work while staying at the Observatoire de la Côte d'Azur, Dept. Cassini, thanks to the "G. Colombo" fellowship of the European Space Agency. We thank for useful comments D.R. Davis, Cl. Froeschlé, A. Milani and M. Šidlichovský.

References

Bendjoya, Ph., Slézak, E., Froeschlé, C., 1991, Astron. Astrophys. 251, 312
Binzel, R.P., Xu, S., 1993, Science 260, 186
Britt, D.T., Tholen, D.J., Bell, J.F., Pieters, C.M., 1992, Icarus 99, 153
Burbine, T.H., Gaffey, M.J., Bell, J.F., 1992, Meteoritics 27, 424
Cellino, A., Zappalà, V., Farinella, P., 1991, Mon. Not. R. astr. Soc. 223, 561
Ceplecha, Z., 1992, Astron. Astrophys. 263, 361
Davis, D.R., Farinella, P., , Paolicchi, P., Weidenschilling, S.J., Binzel, R.P., 1989, In: R.P. Binzel, T. Gehrels, M.S. Matthews (eds.), Asteroids II, Univ. of Arizona Press, Tucson, p. 805
Farinella, P., Davis, D.R., 1992, Icarus 97, 111
Farinella, P., Gonczi, R., Froeschlé, Ch., Froeschlé, C., 1993a, Icarus 101, 174
Farinella, P., Gonczi, R., Froeschlé, Ch., 1993b, Celest. Mech. 56, 287
Froeschlé, Ch., Scholl, H., 1987, Astron. Astrophys. 179, 294
Froeschlé, Ch., Scholl, H., 1992, In: A.W. Harris and T. Gehrels (eds.), Asteroids, Comets, Meteors 1991, Lunar and Planetary Institute, Houston, p. 201

Gaffey, M.J., Bell, J.F., Brown, R.H., Burbine, T.H., Piatek, J.L., Reed, K.L., Chaky, D.A., 1993, Icarus, in press

Hahn, G., Lagerkvist, C.-I., Lindgren, M., Dahlgren, M., 1991, Astron. Astrophys. 246, 603

Knežević, Z., Milani, A., Farinella, P., Froeschlé, Ch., Froeschlé, C., 1991, Icarus 93, 316

Kozai, Y., 1962, Astron. J. 67, 591.

Lemaître, A., Morbidelli, A., 1993, Celes. Mech., in press

McFadden, L., Tholen, D.J., Veeder, G.J., 1989, In: R.P. Binzel, T. Gehrels, M.S. Matthews (eds.), Asteroids II, Univ. of Arizona Press, Tucson, p. 442

Milani, A., Carpino, M., Marzari, F., 1990, Icarus 88, 292

Milani, A., Knežević, Z., 1990, Celest. Mech. 49, 347

Milani, A., Knežević, Z., 1990, Icarus 98, 211

Morbidelli, A., Henrard, J., 1991, Celest. Mech. 51, 169

Morbidelli, A., 1993, Icarus, 105, 48

Öpik, E.J., 1976, Interplanetary Encounters, Elsevier, Amsterdam

Petit, J.-M., Farinella, P., 1993, Celest. Mech., 57, 1

Quinn, T.R., Tremaine, S., Duncan, M., 1991, Astron. J. 101, 2287

Scholl, H., Froeschlé, Ch., Kinoshita, H., Yoshikawa, M., Williams, J.G., 1989, In: R.P. Binzel, T. Gehrels, M.S. Matthews (eds.), Asteroids II, Univ. of Arizona Press, Tucson, p. 845

Scholl, H., Froeschlé, Ch., 1991, Astron. Astrophys. 245, 316

Tholen, D.J., 1989, In: R.P. Binzel, T. Gehrels, M.S. Matthews (eds.), Asteroids II, Univ. of Arizona Press, Tucson, p. 1139

Vilas, F., McFadden, L.A., 1992, Icarus 100, 85

Weidenschilling, S.J., Paolicchi, P., Zappalà, V., 1989, In: R.P. Binzel, T. Gehrels, M.S. Matthews (eds.), Asteroids II, Univ. of Arizona Press, Tucson, p. 643

Wetherill, G.W., 1985, Meteoritics 20, 1

Wetherill, G.W., 1987, Phil. Trans. R. Soc. Lond. A 323, 323

Wetherill, G.W., Williams, J.G., 1979, In: L.H. Ahrens (ed.), Origin and Distribution of the Elements, Pergamon Press, Oxford, p. 19

Williams, J.G., 1969, Secular perturbations in the Solar System, Ph.D. Dissertation, Univ. of California, los Angeles

Williams, J.G., Faulkner, J. 1981, Icarus 46, 390

Wisdom, J., 1983, Icarus 56, 51

Wisdom, J., 1985, Nature 315, 731

Yoshikawa, M., 1987, Celest. Mech. 40, 233

Yoshikawa, M., 1990, Icarus 87, 78

Yoshikawa, M., 1991, Icarus 92, 94

Zappalà, V., Farinella, P., Knežević Z., Paolicchi, P., 1984, Icarus 59, 261

Zappalà, V., Cellino, A., Farinella, P., Knežević Z., 1990, Astron. J. 100, 2030

This article was processed by the author using Springer-Verlag LaTeX A&A style file version 3.